


SCIENTIFIC REPORTS



OPEN

An immune cell spray (ICS) formulation allows for the delivery of functional monocyte/macrophages

Valerie Beneke^{1,2}, Fennja Küster^{1,2}, Anna-Lena Neehus^{1,2}, Christina Hesse^{2,3,4}, Elena Lopez-Rodriguez^{2,4,5}, Kathrin Haake^{1,2}, Anna Rafiei Hashtchin^{1,2}, Juliane Wilhelmine Schott¹, Dorothee Walter^{2,3,4}, Armin Braun^{2,3,4}, Willem F. Wolkers^{2,6} , Mania Ackermann^{1,2} & Nico Lachmann^{1,2}

Macrophages are key cells of the innate immune system and act as tissue resident macrophages (TRMs) in the homeostasis of various tissues. Given their unique functions and therapeutic use as well as the feasibility to derive macrophages *in vitro* from hematopoietic stem cell (HSC) sources, we propose an “easy-to-use” immune cell spray (ICS) formulation to effectively deliver HSC-derived macrophages. To achieve this aim, we used classical pump spray devices to spray either the human myeloid cell line U937 or primary murine HSC-derived macrophages. For both cell types used, one puff could deliver cells with maintained morphology and functionality. Of note, cells tolerated the spraying process very well with a recovery of more than 90%. In addition, we used osmotic preconditioning to reduce the overall cell size of macrophages. While a 800 mosm hyperosmolar sucrose solution was able to reduce the cell size by 27%, we identified 600 mosm to be effective to reduce the cell size by 15% while maintaining macrophage morphology and functionality. Using an isolated perfused rat lung preparation, the combinatorial use of the ICS with preconditioned and genetically labeled U937 cells allowed the intrapulmonary delivery of cells, thus paving the way for a new cell delivery platform.

Macrophages are hematopoietic cells of the myeloid lineage and represent important regulators of the innate immune system as well as key players in tissue homeostasis. Macrophages can be found in a multitude of organs (referred to as tissue resident macrophages; TRMs), for example as microglia in the brain, Langerhans cells in the skin, Kupffer cells in the liver, or as alveolar macrophages (AMs) in the lungs. Especially the latter are of great therapeutic interest, as AMs play an important role in lung tissue integrity by sensing pathogens, regulating immune responses and thereby contributing to tissue homeostasis, protection and repair¹. It was believed for a long time that TRM populations are solely derived from circulating, bone marrow-derived monocytes. However, several recent publications employing genetic fate mapping tools elegantly demonstrate that a number of TRM populations arise early during hematopoietic development from progenitor cells in the yolk sac and fetal liver^{2,3}. Thereafter, these early pre-macrophages seed the fetal tissues and adapt to the specific organ niche⁴. While most TRM populations possess stem cell-like features and are able to maintain their population under homeostatic conditions, also bone marrow-derived monocytes (BMDMs) can replenish resident macrophage pools in case of organ damage or disease. After infiltration of the respective organ, BMDMs are also able to adapt to the instructive tissue environment and gain the functional and transcriptional fingerprint of the resident macrophage population^{5,6}. This exceptional, stem cell-like plasticity renders bone marrow-derived monocytes/macrophages an attractive target population for cell therapeutic approaches.

¹Institute of Experimental Hematology, Hannover Medical School, Hannover, Germany. ²REBIRTH Cluster of Excellence, Hannover, Germany. ³Fraunhofer Institute for Toxicology and Experimental Medicine (ITEM), Hannover, Germany. ⁴Biomedical Research in Endstage and Obstructive Lung Disease (BREATH), German Center for Lung Research, Hannover, Germany. ⁵Institute of Functional and Applied Anatomy, Hannover Medical School, Hannover, Germany. ⁶Institute of Multiphase Processes, Leibniz Universität Hannover, Hannover, Germany. Valerie Beneke and Fennja Küster contributed equally. Correspondence and requests for materials should be addressed to N.L. (email: lachmann.nico@mh-hannover.de)

Received: 8 June 2018

Accepted: 18 October 2018

Published online: 02 November 2018

Given the important role of TRMs in organ homeostasis, macrophage dysfunction has been related to a variety of diseases. As an example, impairment of AMs has been shown to interfere with the surfactant metabolism, causing the rare pulmonary disease known as pulmonary alveolar proteinosis (PAP). The hereditary form of PAP (herPAP) is caused by mutations in the granulocyte-macrophage colony-stimulating factor (GM-CSF) receptor genes, resulting in disturbed alveolar macrophage development and function. As a consequence, herPAP patients suffer from massive protein accumulation in the lungs, and life-threatening respiratory insufficiency^{7,8}. In addition to the development of herPAP, malfunctional AMs have also been associated with other respiratory diseases e.g. cystic fibrosis⁹. To establish a novel and cause directed therapy, we and others recently exploited the therapeutic potential of BMDMs as a novel cell-based treatment approach for herPAP. In these proof-of-concept studies, a single intra-pulmonary administration of stem cell-derived macrophages resulted in life-long therapeutic benefit in transplanted animals, thereby introducing a new concept of cell therapy using mature macrophages^{10,11}.

To further translate the intra-pulmonary transplantation of macrophages into clinical practice, an “easy-to-use” cell transfer system is warranted. Here, a cell application system which would allow for a local cell administration, e.g. directly into the lung microenvironment, is of high therapeutic value as several studies have suggested superior effects of local compared to systemic administration of macrophages. With respect to clinical translation, the delivery of macrophages into the lung environment may be accomplished via the use of bronchoscopy instruments. This scenario however, represents a quite invasive process and requires general anesthesia.

Although bronchoscopy instruments are already regularly used in the clinics, we aim to establish an alternative and to provide a proof-of-concept study for an immune cell spray (ICS) formulation, which is able to locally deliver macrophages. Given the pre-clinical efficacy of intra-pulmonary macrophage transplantation in herPAP, an ICS may also be applied to deliver macrophages for the treatment of other pulmonary diseases. In addition to the pulmonary application, the development of an ICS would open a broad range of applications also for other tissues (e.g. ectopic use on skin). Indeed, a cell spray formulation has been applied in the past for the delivery of skin cells to burn wounds^{12,13}. Given the important role of infiltrating bone marrow-derived monocyte/macrophages and resident Langerhans cells in wound healing and as a first line of cellular immunity, an ICS may also be used to deliver macrophages ectopically onto the skin in order to (i) support wound healing, (ii) combat/prevent wound infections, or (iii) reduce scar formation¹⁴.

With the objective to develop an ICS for the local administration of macrophages either onto the skin or directly into the lung environment, we demonstrate the efficient use of a classical pump spray device to spray myeloid cell lines as well as primary murine BMDMs. Importantly, the cells showed a high viability as well as maintained functionality after the spraying process. To further develop the ICS for the administration of macrophages into the bronchoalveolar space, we used hyperosmolar conditions to reduce the cell size of macrophages. In the present work, we were able to identify optimal conditions to reduce the cell size of macrophages while maintaining important functional characteristics. Moreover, we demonstrate the efficient local administration of shrunken cells into a perfused rat lung via a micro sprayer device, paving the way for macrophage cell spray formulations.

Results

Development of an immune cell spray (ICS) formulation. In order to develop an immune cell spray (ICS) formulation, we used classical pump spray devices (Fig. 1a,b) and investigated the feasibility to spray either human hematopoietic cell lines or primary murine bone marrow-derived macrophages. In a first set of experiments, we used the human myeloid cell lines K562 or U937 and tested a variety of spraying devices for their applicability to deliver myeloid cells. With respect to practicability, sterility and cleaning procedures of the individual devices, we identified a classical pump spray/nozzle configuration (Fig. 1b) (brown glass, volume 20 mL, spray volume approx. 50 μ L, company Rixius AG, Mannheim Germany) to be most promising. This spray device has been used for further studies.

In order to evaluate the viability of U937 cells after the spraying process, at least 1 mL of a cell solution containing 6 or 12 $\times 10^6$ cells/mL was filled into the spray device and then sprayed into a falcon tube. Using a cell density of 6 $\times 10^6$ cells/mL, 2.1 $\times 10^5 \pm 3.8 \times 10^4$ or 3.2 $\times 10^5 \pm 1.9 \times 10^4$ (mean \pm SEM) viable cells per puff could be detected for U937 or K562 cells respectively (Fig. 1c and Supp. Fig. 1a). After increasing the concentration of the cell solution to 12 $\times 10^6$ cells/mL approximately twice as many cells per puff could be detected for both cell types (Fig. 1c and Supp. Fig. 1a). To further assess the dynamics of the spraying process, we quantified cell numbers after repetitive spraying of U937 and K562 cell solutions, showing that the number of cells rise proportionally with each puff (Fig. 1d and Supp. Fig. 1b). Of note, given a spraying volume of 42.23 \pm 7.2 μ L (mean \pm SEM), the expected cell dose would range approx. 3 $\times 10^5$ cells/puff for a cell suspension containing 6 $\times 10^6$ cells/mL. As a next step, we evaluated the cell viability of sprayed cells. Here, irrespective of the cell density used, we observed an overall viability of >90% of sprayed cells (97.97 \pm 0.34% and 96.44 \pm 1.06% for U937 cells, 6 and 12 $\times 10^6$ cells/mL, respectively and 96.00 \pm 1.53% and 99.09 \pm 0.28% for K562 cells, 6 and 12 $\times 10^6$ cells/mL, respectively, mean \pm SEM) (Fig. 1c and Supp. Fig. 1a). The viability of U937 cells following the spraying process was further confirmed by the detection of apoptotic cells using propidium iodide (PI) staining. Using flow-cytometric analysis, we could not detect any significant differences in the percentage of PI⁺ cells before and 1 hour after the spraying process (Fig. 1e).

Delivery of macrophages as a cell spray formulation does not influence viability or functionality. After we successfully established the ICS, we next evaluated the possibility to spray macrophages which have been previously differentiated from murine bone marrow. Similar to the afore mentioned studies, we first concentrated on the feasibility to spray bone marrow-derived macrophages (BMDMs) (3 $\times 10^6$ cells/mL) and analyzed their phenotype and functionality before and after the spraying process. Using the same spray device, we observed a high viability of primary macrophages 1 hour after the spraying process, which was very similar to non-sprayed control cells (Fig. 2a). Moreover, we confirmed a macrophage like phenotype of the sprayed

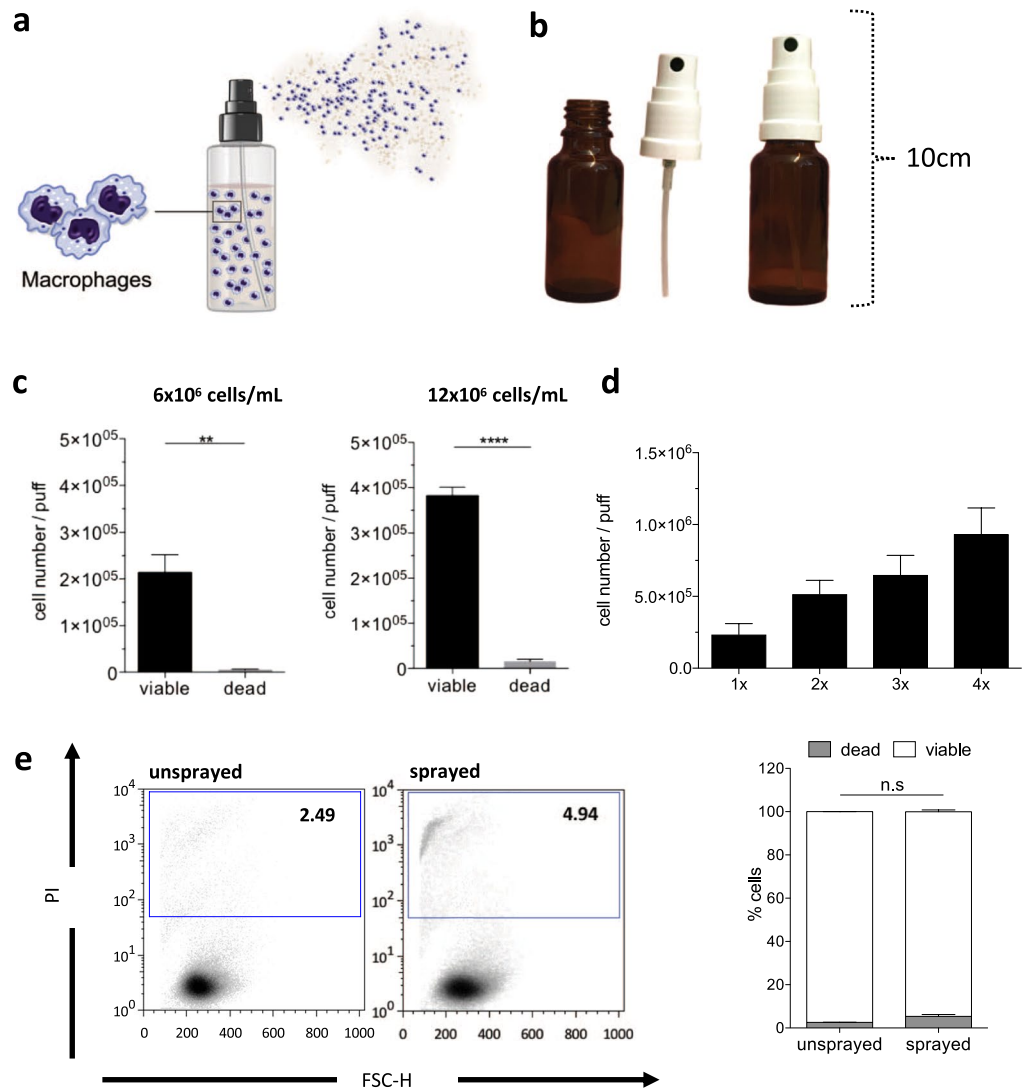


Figure 1. Spraying of U937 cells. **(a)** Schematic overview of the cell spraying procedure and **(b)** image of the pump spray devices used for our studies. **(c)** Numbers of viable and dead U937 cells after the spraying process, analyzed via trypan blue staining. Initial concentrations of 6×10^6 cells/mL (left) and 12×10^6 cells/mL (right) were used (significance of $**P < 0.01$ or $****P < 0.0001$ by two-tailed paired student t-test, $n = 3-6$ mean \pm SEM). **(d)** Cell numbers/puff at a cell concentration of 6×10^6 cells/mL ($n = 6$, mean \pm SEM). **(e)** Evaluation of cell viability after the spraying process by propidium iodide (PI) staining (Left: Representative flow cytometry analysis. Right: Quantification of cell viability $n = 3$ mean \pm SEM). (n.s.: denotes not significant. Statistical analysis: analyzed by two-way repeated measurements (RM) ANOVA with Bonferroni post-hoc-test).

macrophages by cytospin staining as well as flow cytometric analysis (Fig. 2b,c). Of note, evaluating different cytospin preparations ($n = 3$), we could observe a reduction in the size of macrophages by approx. 21% following the spraying process compared to the non-sprayed counterparts. Following the spraying process, macrophages maintained typical surface markers and stained positive for CD45.1, CD11b, and F4/80 (Fig. 2c). Even more importantly, we could also see maintained functionality of macrophages after the spraying process. Using a pHrodo labeled *E. coli* bioparticles phagocytosis assay, macrophages after the spraying process were able to phagocytose bioparticles as efficient as non-sprayed control cells (Fig. 2d). Moreover, the spraying process had no influence on the ability of macrophages to upregulate MHCI in response to $IFN\gamma$ stimulation (Fig. 2e).

Macrophage cell size reduction by applying hyperosmolar sugar solutions. Having proven the feasibility of the ICS, we next aimed to further optimize the macrophage spray formulation to make it suitable for the delivery of cells directly into the airways. Given the considerable large size of macrophages (approx. 15 μ m diameter)¹⁵, we investigated the effect of hyperosmolar sucrose solutions to temporary reduce the overall cell size of macrophages. The reduction of the cell size is of particular importance as the size of particles has been shown to be a crucial parameter for intra-pulmonary drug delivery¹⁶.

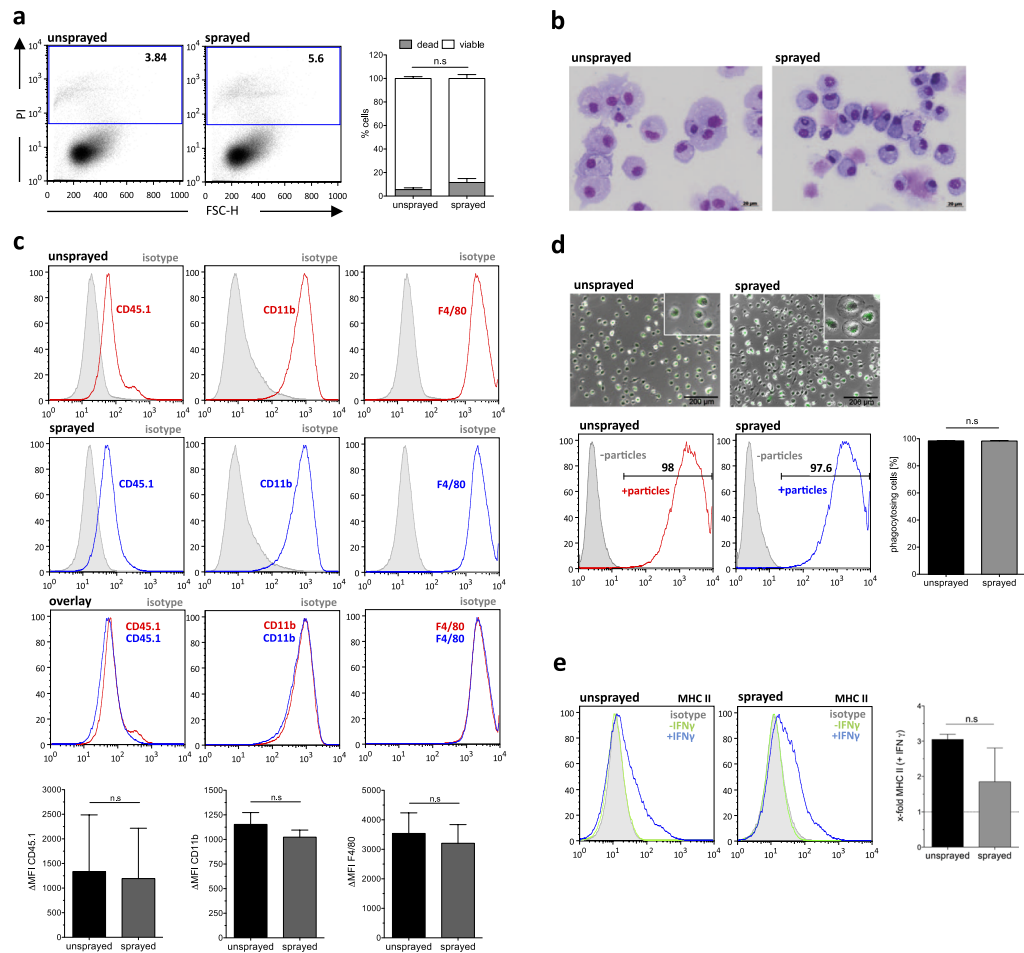


Figure 2. Functionality of bone marrow (BM)-derived macrophages after spraying. **(a)** Flow cytometric analysis of cell viability by propidium iodide (PI) staining of unsprayed and sprayed BM-derived macrophages (Left: representative images, right: quantification of $n = 3$, mean \pm SEM). **(b)** Papanheim staining of cytopsin preparations of sprayed and unsprayed BM-derived macrophages (scale bar: 20 μm) **(c)** Flow cytometric analysis of CD45.1, CD11b and F4/80 expression of unsprayed and sprayed BM-derived macrophages. Overlays of representative histograms; grey filled line: isotype, red/blue line: surface marker of unsprayed or sprayed macrophages. Lower panels: Delta mean fluorescent intensity (MFI) of surface marker expression of unsprayed and sprayed BM-derived macrophages (delta MFI was calculated by subtracting isotype (negative) MFI from surface marker (positive) MFI; $n = 3$, mean \pm SEM). **(d)** Phagocytic activity of unsprayed and sprayed BM-derived macrophages. Upper panels: representative fluorescent microscopy images of BM-derived macrophages 2 hours after incubation with pHRedo *E. coli* BioParticles (scale bar: 200 μm). Lower panel: Representative flow cytometric analysis (grey filled line: cells without *E. coli* BioParticles, red line: unsprayed cells with *E. coli* BioParticles, blue line: sprayed cells with *E. coli* BioParticles) and quantification of $n = 3$ (mean \pm SEM). **(e)** Analysis of MHC-II surface marker expression by flow cytometry of unsprayed and sprayed BM-derived macrophages before and after stimulation with IFN γ . Left: Representative histograms (grey filled line: isotype, green line: non-stimulated control, blue line: IFN γ stimulated) and right: Quantification of the fold change in MFI, $n = 3$, mean \pm SEM). (n.s. denotes not significant. Statistical analysis: **a**: two-way repeated measurements (RM) ANOVA with Bonferroni post-hoc-test; **(c–e)** two-tailed paired student t-test).

When applying hyperosmolar D(+)-sucrose solutions (600, 800 and 1000 mosm) to murine BMDMs or U937 cells, we observed morphological changes already within 15 min after incubation as indicated by a change in forward/sideward scatter (FSC/SSC) properties (Fig. 3a and Supp. Fig. 2a). Of note, the decrease in FSC values was concentration dependent, indicating a reduction of cell size most likely explained by the osmotic efflux of water (Fig. 3a). The same observation could be made in treated U937 cells, showing the maximal osmotic effect using 1000 mosm sucrose solutions (Supp. Fig. 2a). To further verify this observation, we measured the size of treated cells after 1 hour in hyperosmolar solutions by light microscopy and subsequent ImageJ analysis. Similar to the flow cytometry data, we could observe a significant decrease of the cell area in all three hyperosmolar conditions of primary murine BMDMs (Fig. 3b) as well as U937 cells (Supp. Fig. 2b). Applying sucrose solutions of 600, 800, or 1000 mosm to BMDMs, we observed a reduction in the cell area by 15.5%, 26.9%, and 26.0% (control: 155.7 μm^2 , 600 mosm: 131.6 μm^2 , 800 mosm: 113.9 μm^2 , 1000 mosm: 115.2 μm^2 ; all mean values), respectively. Similarly, preconditioning of U937 cells led to cell size reduction of 17.1%, 27.4% and 34.8% (control: 113.8 μm^2 ,

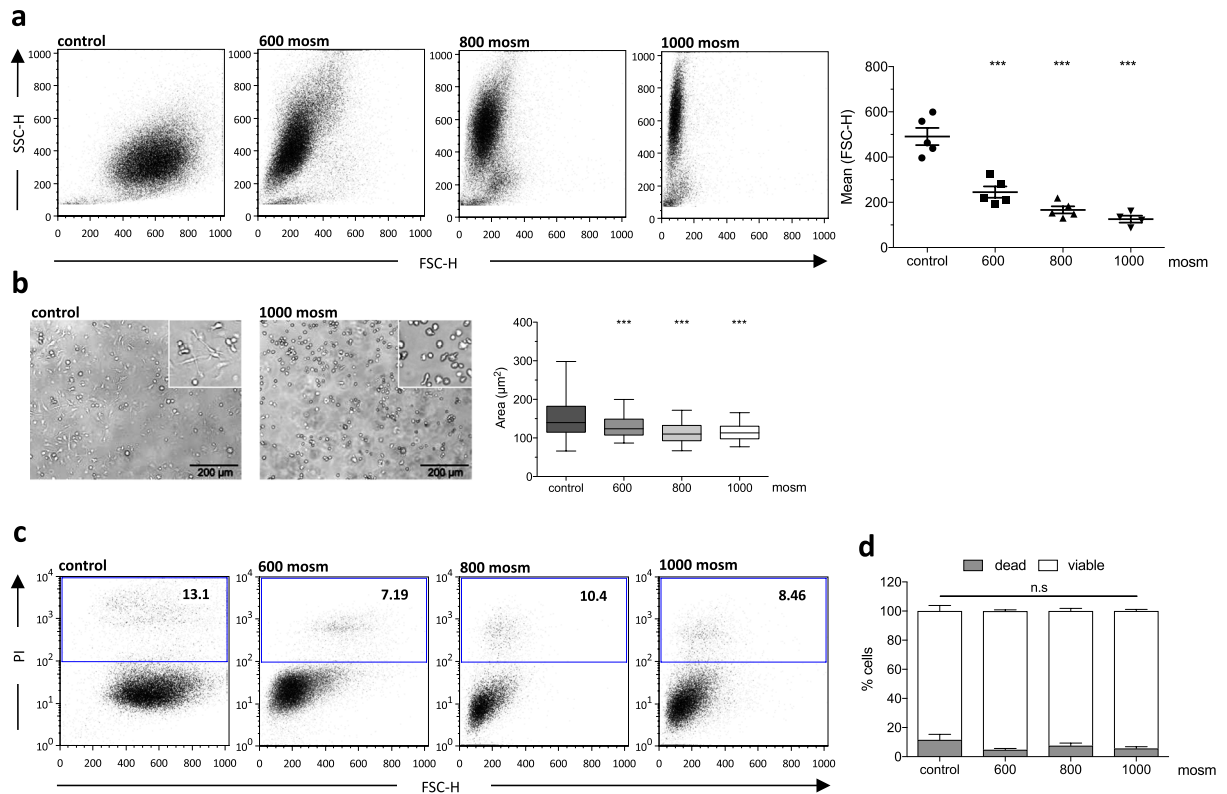


Figure 3. Shrinking of BM-derived macrophages using hyperosmolar solutions. **(a)** Flow cytometric analysis using FSC-H/SSC-H plot discrimination (left panel) and mean of FSC-H (right panel) for control (PBS) and hypertonic solutions ($n = 4-5$, biological repeats, mean \pm SEM, significance of $***P < 0.001$ by one-way ANOVA with Tukey's post-hoc-test). **(b)** Representative brightfield images of BM-derived macrophages after incubation in control medium and 1000 mosm solution (scale bar: 200 μm) and ImageJ analysis of cell area (right panel; $n = 105-482$, technical repeats, mean with 95% CI, significance of $***P < 0.001$ by one-way ANOVA with Tukey's post-hoc-test). **(c)** Flow cytometric analysis of cell viability by propidium iodide (PI) staining of macrophages after incubation (60 min) in control (PBS) and hypertonic solutions. **(d)** Quantification of cell viability after incubation in control (PBS) and hypertonic solutions ($n = 4-5$ mean \pm SEM). (n.s.: denotes not significant analyzed by two-way ANOVA with Bonferroni post-hoc-test).

600 mosm: 94,34 μm^2 , 800 mosm: 82,63 μm^2 , 1000 mosm: 74.26 μm^2 ; all mean values) respectively (Fig. 3b and Supp. Fig. 2b). Importantly, treated murine BMDMs as well as U937 cells tolerated the incubation in hyperosmolar solutions very well indicated by less than 12% dead cells after 60, or 15 minutes of incubation, respectively (Fig. 3c,d and Supp. Fig. 2c,d).

Murine BMDMs remain functionally and phenotypically normal following temporary shrinking.

After demonstrating efficient size reduction of primary murine BMDMs and U937 cells by incubation in hyperosmolar sugar solution, we evaluated the phenotype and functionality of the treated BMDMs. This is of great importance, as maintained functionality of shrunken macrophages would be a prerequisite for future clinical translation. Flow cytometric analysis revealed a maintained surface marker profile of CD45.1⁺/CD11b⁺/F4/80⁺ 1 hours post incubation in 600, 800 or 1000 mosm hypertonic solutions. Moreover, no significant change in mean fluorescent intensity (MFI) values could be observed, indicating no effect on cell surface marker expression (Fig. 4a,b). Of note, when cells have been pretreated in hypertonic solutions and subsequently be maintained in 300 mosm physiological conditions, a normal characteristic cell morphology as well as normalized overall cell size was observed (Fig. 4c). We next evaluated the phagocytic capacity of cells that were first cultured in hypertonic solutions and then treated with physiological conditions to become normal. In these assays, we observed efficient and steady phagocytosis for cells previously shrunk in a 600 mosm sugar solution. However, BMDMs incubated in higher concentrated sugar solutions (800 mosm and 1000 mosm) showed an impaired phagocytic potential, indicating a detrimental effect on the functionality by the hyperosmolaric treatment (Fig. 4d). Primary BMDMs also tolerated exposure to hyperosmolaric solutions (600 mosm) followed by the spraying process. The so treated BMDMs were able to efficiently phagocytose *E. coli* bioparticles equally as efficient as BMDMs cultured in control physiological conditions (Supp. Fig. 3).

Local administration of GFP-labeled U937 cells into isolated perfused rat lungs. To further prove our ICS concept to locally deliver monocyte/macrophages directly into the airways, we have performed proof-of-concept studies utilizing a Microsprayer[®] Aerosolizer device for rats (model IA-1B-R, PennCentury)

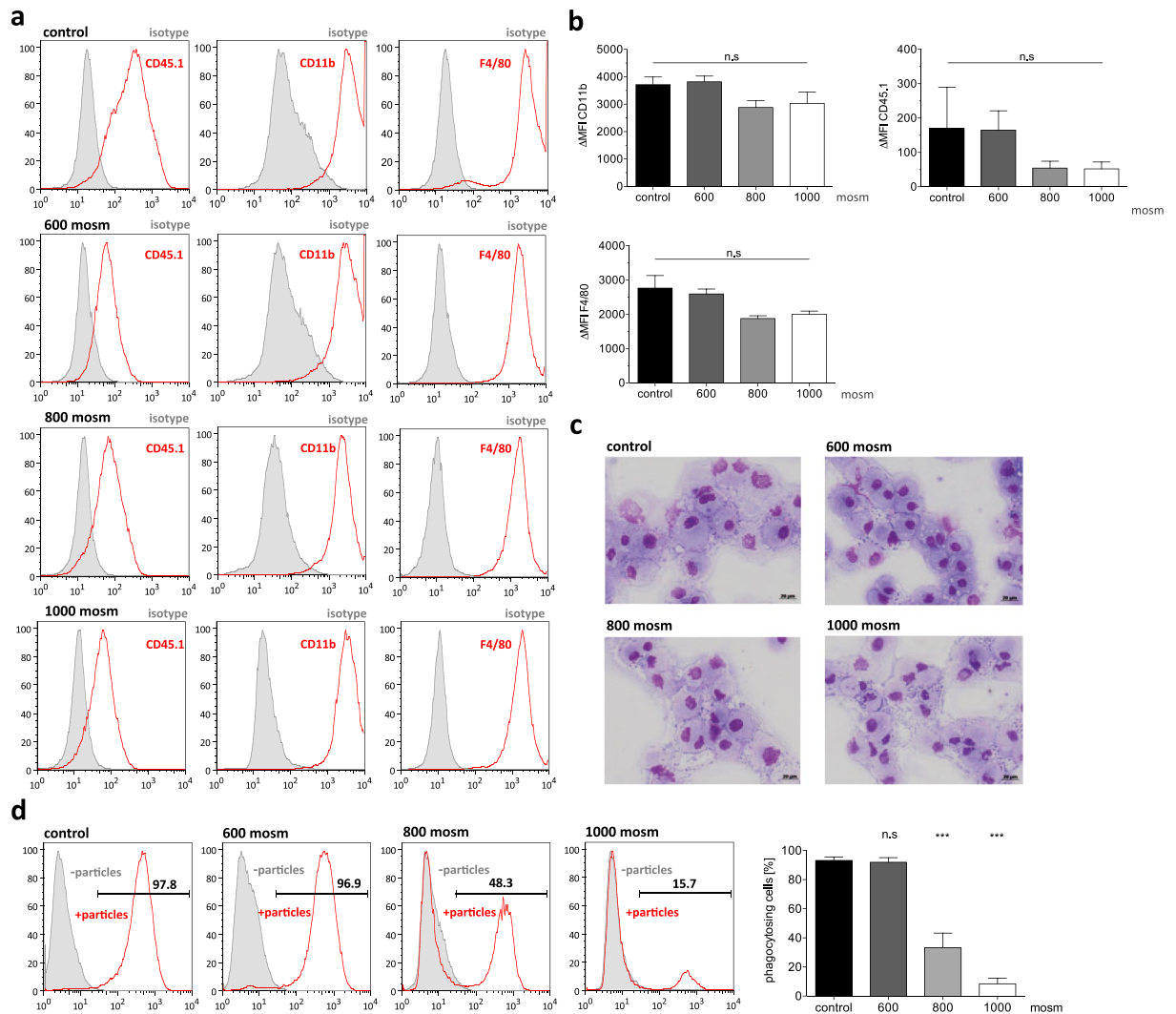


Figure 4. Functional analysis of BM-derived macrophages after incubation in hyperosmolar solutions. **(a)** Flow cytometric analysis CD45.1, CD11b and F4/80 surface marker expression on BM-derived macrophages after incubation in control (PBS) and hypertonic solutions (grey filled line: isotype, red line: surface marker). **(b)** Delta mean fluorescent intensity (MFI) of surface marker expression (delta MFI was calculated by subtracting isotype (negative) MFI from surface marker (positive) MFI; $n = 3$ biological repeats, mean \pm SEM, n.s.: not significant by one-way ANOVA with Tukey's post-hoc-test). **(c)** Cytopins of BM-derived macrophages after incubation in control (PBS) and hypertonic solutions (scale bar: 20 μ m). **(d)** Phagocytic activity of unsprayed and sprayed BM-derived macrophages. Left: Representative flow cytometric analysis (grey filled line: cells without *S. aureus* BioParticles, red line: cells with *S. aureus* BioParticles) and quantification of $n = 3$ (mean \pm SEM) (n.s. denotes not significant, significance of *** $P < 0.001$ by one-way ANOVA with Tukey's post-hoc-test).

in combination with the isolated perfused rat lung (IPL) model¹⁷ (IPL-2, Harvard Apparatus, Holliston, MA, USA). In order to visualize the cells after transplantation, we employed genetically labeled U937 cells previously transduced with lentiviral vectors expressing GFP from a CMV early enhancer/chicken β -actin (CAG) promoter (kindly provided by Daniela Paasch, Hannover Medical School).

To ensure efficient tracking, we first confirmed strong GFP expression in the transgenic U937 cells (Fig. 5a,b). In order to reach the lower airways in our IPL model, we subjected the transduced U937 cells to hyperosmolar preconditioning using the afore evaluated 600 mosm sugar solution. As a next step, we applied a cell solution of 4×10^6 cells/300 μ L directly into the trachea of the rat IPL using the Microsprayer device. During and directly after cell administration, a total of 10 deep inspiratory breaths were performed in order to ensure macrophage deposition into distal airway spaces. Respiratory parameters were evaluated simultaneously and revealed a short-term reduction of airflow, which was reflected in a slight increase in lung resistance (R_L). This increase was restored to baseline levels after performance of the deep breaths. In addition, a reduction of dynamic lung compliance (C_{dyn}) by 75% was found. These effects could not be reversed by performance of the deep breaths and lasted throughout the subsequent experimental time of 1 hour. Using the afore mentioned technique, a cleared air-inflated and

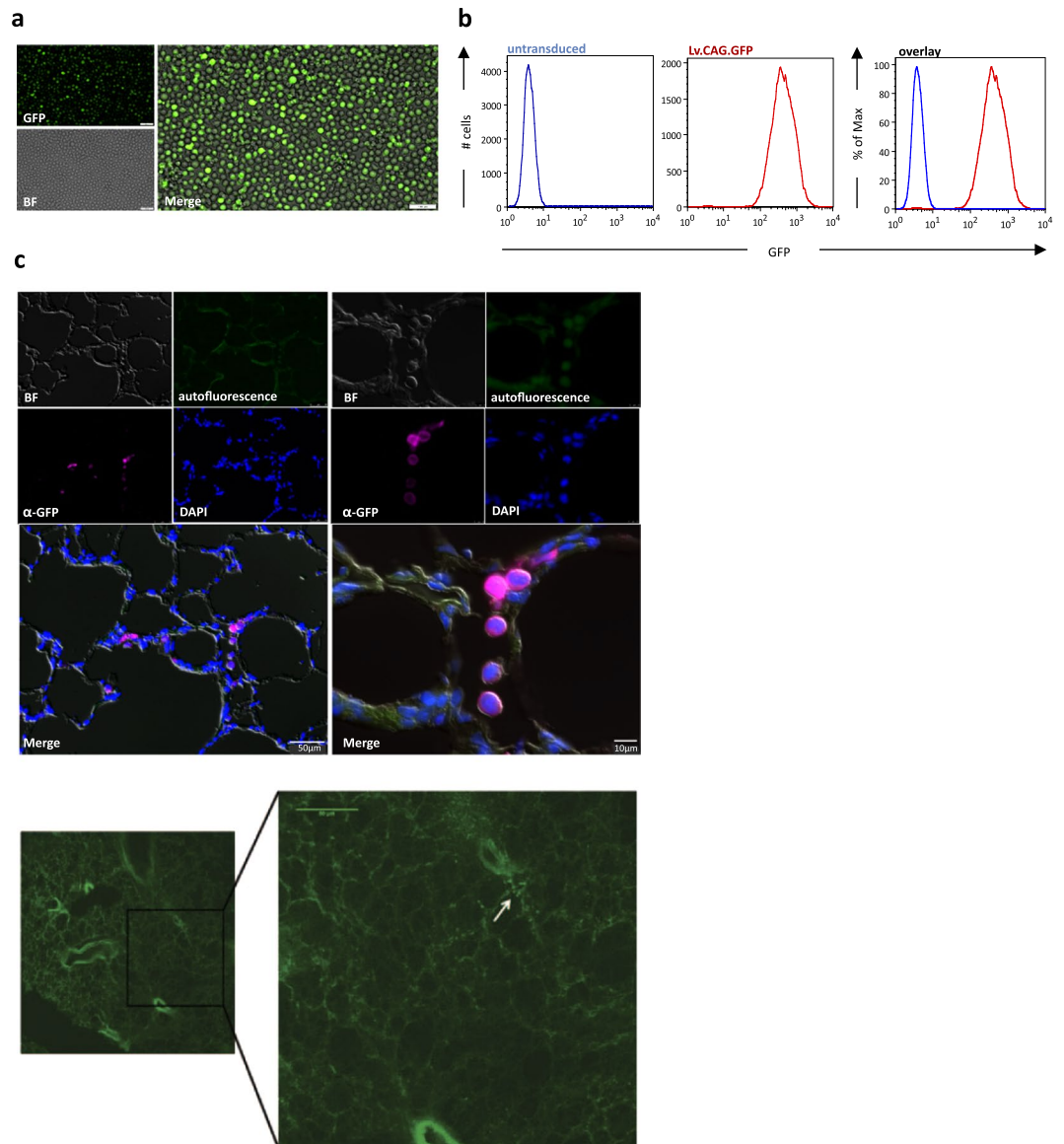


Figure 5. Local administration of GFP-labeled U937 cells into isolated perfused rat lung (IPL) (a) Representative fluorescent microscopy images of U937 cells transduced with lentiviral vectors expressing GFP from a CMV early enhancer/chicken beta-actin promoter (Lv.CAG.GFP) (scale bar: 100 μ m; BF: brightfield) (b) Flow cytometric analysis of GFP expression in Lv.CAG.GFP transduced U937 cells (blue line: untransduced cells, red line: cells transduced with Lv.CAG.GFP) (c) Analysis of U937 cell localization after application to the IPL. Upper panels: Immunofluorescence staining of cryostat sections generated from the lobus accessorius of the IPL (left: scale bar 50 μ m, right: scale bar 10 μ m), U937 cells were detected by anti-GFP antibody staining. Lower panel: Representative images of horizontal 2-Photon microscopy of lobus accessorius (right: scale bar: 60 μ m).

fixed lobus accessorius was observed in a scanning horizontal 2-Photon microscope where cell-like bright green structures can readily be localized in alveolar spaces (Fig. 5c). A closer look using specific fluorescence immunostaining against GFP revealed GFP-positive cells (of approx. 8–10 μ m diameter) not only at the air-spaces but also in close contact with alveolar epithelium (Fig. 5c). Therefore, cells appear to reach the alveolar distal spaces of the lungs.

Discussion

In summary, we introduce an immune cell spray (ICS) formulation which would allow for the local delivery of macrophages to skin or lung respectively. We demonstrate that different myeloid cell lines as well as primary murine BMDMs can be delivered as a cell spray employing classical pump spray devices, survive the spraying process, and remain functional afterwards.

The so developed ICS formulation could in principle be applied to supply macrophages into different tissues e.g. into the lung environment or onto skin wounds. Indeed, cell spray formulations delivering skin cells to burn

wounds were already able to prove feasibility, demonstrating profound clinical effects while reducing the amount of donor skin needed per wound area^{18,19}. Given the regulatory role of monocyte/macrophages and Langerhans cells in wound healing as well as tissue homeostasis, the supplementary use of macrophages in such cell spray compositions might be of advantage. Alternatively, macrophages also represent an important part of the innate immune system with strong antimicrobial activities²⁰. Thus, a macrophage-based cell spray formulation may be used in wound healing and to counteract bacterial infections. Bacterial infections associated with burn wounds, represent a clinical challenge and can cause severe clinical complications²¹. This becomes even more problematic if the pathogens are refractory to current standard antibiotic therapy. In such a clinical scenario, a combined therapeutic approach using a cell spray formulation of macrophages and fibroblasts/keratinocytes together with current care medicine may be beneficial and might offer new perspectives to fight infections and support wound healing. Following this hypothesis, a recent study already investigated a monocyte/macrophage-based cell therapy applying macrophages via a biomimetic hydrogen scaffold to cutaneous wounds. Using M-CSF-derived bone marrow macrophages, the authors could demonstrate accelerated wound healing in wild type as well as diabetic mice²².

In addition to the use of a macrophage-based ICS formulation to improve wound healing, the envisioned ICS may also be used to locally apply macrophages directly into the lung environment. In contrast to the administration of macrophages onto the skin, a direct pulmonary transfer of cells may require a smaller size of the cells in order to reach the small bronchioles and alveoli. Considering the lung architecture, the upper respiratory tract with the nasopharynx, trachea, and large bronchi is responsible for the filtration and removal of 70–90% of particles¹⁶. To circumvent the clearance of cells and to further reach the lower respiratory tract, the envisioned size of the particles/cells should ideally be less than 5 μm , if applied by oral inhalation^{16,23,24}. In our studies, we reached a cell size of <10 μm for U937 and approx. 12 μm for BMDMs, however we did not reach the critical 5–8 μm size. Here, more intensified studies with improved protocols for cell shrinking using hyperosmolar sugar solutions or even salt solutions have to be performed.

Given our ICS proof-of-concept study, short term bronchoscopy intervention or even endotracheal intubation may be combined with the use of macrophages in order to deliver the cells into the lower airways and to establish a clinically applicable cell administration procedure. While macrophages are generally considered to be of 13–20 μm (in suspension)^{15,25}, we here evaluated the incubation of macrophages in a hyperosmolar sugar solution as a method to reduce cell size. To achieve this aim, we used a sucrose gradient to gently reduce cell size. Cell volume response to anisotonic solutions can be described by the Boyle-van't Hoff law. However, cells only respond as linear osmometers in a defined osmotic range within the osmotic tolerance limits of the cell²⁶. Applying different sucrose solutions with 600, 800, or 1000 mosm, we were able to efficiently reduce the cell size by 15–26% for BMDMs or 17–35% for U937 cells (calculated to the initial size). Although we used a hypertonic sucrose solution instead of a salt solution to keep the stress to the cells as low as possible, we observed an impairment in functionality after incubation of primary macrophages with 800 and 1000 mosm. However, when applying the 600 mosm solution we observed a significant size reduction while maintaining the functionality of the cells. It could well be that with shorter exposure times, cells may be able to survive exposure to higher hyperosmolar solutions while maintaining their functionality. Although we performed proof-of-concept experiments demonstrating an efficient spraying of previously shrunk cells (600 mosm) into a rat lung explant culture, it remains to be elucidated whether the reduction in cell size would be sufficient to allow the cells to reach the lower respiratory tract. In our explanted rat perfusion lung model, we directly applied the cells into the upper airways via a microsyringe device, bypassing the nasopharynx section. While our studies represent a proof-of-concept study, further experiments which would address the feasibility of an e.g. cell nebulizer would be warranted to investigate nasal vs. oral aerosol inhalation. While the process of spraying also has an effect on macrophages alone (determined by cytospin preparations), the combinatorial effect of spraying and shrinking of macrophages needs to be investigated in more detail. Of note, these values are derived from cytospin preparations and therefore might not represent the actual cell size of living cells in suspension. As an alternative method to the temporal hyperosmotic preconditioning, also the use of freeze-drying preservation methods might be applied. Although freeze-drying of mononuclear cells has been proven feasible^{27,28}, further improvements have to be made with respect to cell viability before using macrophages. Similarly, also further improvements in the cell delivery techniques have to be made. In our proof-of-concept study we have used a pump and nozzle configuration, which might not allow for the production of droplets in appropriate sizes for uniform lung deposition. As an alternative, pressurized metered-dose inhalers (pMDIs), “dry powder” inhalers (DPIs), or even nebulizers²⁹ could be combined with modified macrophages in order to develop a clinically applicable ICS.

In order to establish the proof-of-concept for the ICS, we used primary macrophages from murine bone marrow. While use of the ICS in combination with murine cells has been proven feasible, human macrophages have to be investigated next. Whereas an allogeneic or even an autologous approach (e.g. a hematopoietic stem cell (HSC) based gene therapy combined with a macrophage-differentiation approach) might be an option, a promising alternative is represented by the use of human induced pluripotent stem cell (iPSC) technology. Previously, different studies have already proven the generation of macrophages from human and murine iPSC^{30–32}. Human iPSC macrophages demonstrate high phenotypical and functional similarities to BMDMs and, even more important, can engraft into the lung in humanized mouse models and gain the transcriptional and functional fingerprint of the resident population^{30,33}. Further studies employing human macrophages, which are either generated from adult type HSC or pluripotent stem cells in combination with the ICS may allow for new cell-based therapies and to apply macrophages as an off the shelf cell-product.

Methods

Cell culture. The human cell lines U937 and K562 were cultured in RPMI 1640 (Thermo Fisher Scientific, Waltham, MA, USA) supplemented with 10% fetal calf serum (FCS, Biochrom, Berlin, Germany) and 1% penicillin/streptomycin (Thermo Fisher Scientific).

Isolation of murine bone marrow and macrophage differentiation. The procedure of isolation of murine bone marrow/rat lung were in accordance with the German Animal Welfare Legislation (§4, TierSchG) and approved by the local Institutional Animal Care and Research Advisory Committee and permitted by the Lower Saxony State Office for Consumer Protection and Food Safety. While no experiments on living animals was performed, no approval from the local ethical committee was needed, which is in accordance with institutional guidelines. For isolation and cultivation of murine bone marrow-derived macrophages, femur, tibiae of B6.SJL-*Ptprca*^o *Peprca*^b/BoyJ (CD45.1) (purchased from animal facility ZTL Hannover Medical School) mice were flushed with PBS supplemented with 2% FCS and 0.5% EDTA (Omnilab, Gehrden, Germany) and centrifuged at 500 x g for 5 minutes. Lysis of erythrocytes was performed using red cell lysis buffer (156 mM NH₄Cl, 46 mM KHCO₃, 0.5 mM EDTA) for 2 minutes. Purified precursor cells were cultivated and differentiated in RPMI 1640 + 30% L929-cell conditioned medium (LCCM) as a source for macrophage colony-stimulating factor for 7 days.

Isolated Perfused Rat Lung model (IPL). To assess the deposition of macrophages in the lower respiratory tract, an isolated perfused rat lung (IPL) model was used. As a donor animal, a female wistar rat (CrI:Wi (Han)) (Charles River Laboratories in Sulzfeld, Germany) was used. The IPL was performed as previously described by Uhlig (Uhlig, S. (1998) “*The isolated perfused rat lung. Methods in Pulmonary Research. 1st, pp. 29–55, Basel, Birkhäuser*”) and Fischer *et al.*¹⁷. In brief, isolated lungs (materials during isolation were perfused in a recirculating system with constant pressure (12 cmH₂O). This resulted in a flowrate of 27.8 mL/min. Ventilation was switched from positive to negative pressure (end-inspiratory: –7.5 cm H₂O; end-expiratory: –3.0 cm H₂O; inspiratory oxygen fraction FiO₂ = 0.21) after the isolated organ was placed into the artificial thoracic chamber. Ventilation frequency was set to 80 breaths/min and the ratio of inspiratory to expiratory duration to 1:1. An equilibration period of 30 min was provided before administration of the cells. Every 5 minutes, a hyperinflation (21 cm H₂O) was performed to re-open atelectatic lung areas and enhance release of surfactant.

Spraying of cells. Spraying of cells was performed utilizing a pump spray bottle made out of glass (brownglass, volume 20 mL, white plastic finger sprayer cap, spray volume approx. 50 µL company Rixius AG, Mannheim Germany). One mL of cell suspension was transferred into the flask to ensure effective spraying. The cell suspension was sprayed into a 15-mL falcon tube in multiple spraying rounds to yield sufficient cell numbers for following analysis. Evaluation of cell number and cell viability after spraying was performed using trypan blue (Thermo Fisher Scientific) exclusion.

Exposure to hyperosmolar solutions. To shrink the cells, hypertonic solutions ranging from 600 mosm to 1000 mosm were prepared by adding the corresponding amount of D(+)-saccharose to isotonic PBS (300 mosm). For osmolarity experiments, 5 × 10⁵ cells were incubated in 2 mL of hypertonic solutions for 15 minutes or 1 hour to examine cell viability, FACS analysis and phagocytosis, respectively.

Flow Cytometric Analysis. Analysis of surface marker expression was performed as described before³⁰. For antibody staining of shranked cells, cells were kept in hypertonic solutions supplemented with 2% FCS. Antibodies were used as follows: CD11b-PE (12-0112-82), CD45.1-APC (17-0453), F4/80-APC (17-4801-80), MHC-II (I-A/I-E)-APC (17-532-81), isotype controls: rat IgG2ak-APC (17-4321-41), mouse IgG2bk-PE (12-4031-81) (all from eBioscience). Propidium iodide (PI; Sigma-Aldrich, St. Louis, MO, USA) was diluted 1:100 and added directly before FACS analysis.

For measurement of MHC Class II upregulation after IFN γ stimulation macrophages were either left unstimulated or stimulated with 25 ng/mL IFN γ for 24 hours. Flow cytometry was performed using FACSCalibur (BD) and further analysed using FlowJo V8 (Tree Star).

Cytospins. For cytopins, 3 × 10⁴ cells were centrifuged on object slides for 7 minutes at 600 x g and dried overnight. Slides were stained in May-Grünwald staining solution (0.25% (w/v) in methanol) for 5 minutes, followed by 20 minutes in 5% of Giemsa azur-eosin-methylene blue solution (0.4% (w/v)) in methanol, working solution was 0.02%) and washed extensively in aqua dest.

Phagocytosis assay. For assessment of phagocytosis, 1 × 10⁵ cells were seeded in 12-well plates in standard medium. After >12 hours of settling, cells were incubated for 2 hours with pHRedo Green *E. coli* or pHRedo Red *S. aureus* BioParticles (Thermo Fisher Scientific) at a concentration of 1:20. Phagocytosis was performed in phenol-free RPMI 1640 (Thermo Fisher Scientific) supplemented with 10% FCS, 2% HEPES (AppliChem, Darmstadt, Germany), 1% L-glutamine (Invitrogen, Darmstadt, Germany) and 10 pg/mL murine M-CSF (R&D Systems, Minneapolis, MN, USA). Subsequently, cells were washed extensively, and the amount of incorporated BioParticles was evaluated by flow cytometry.

ImageJ analysis. Determination of cell size was carried out using ImageJ2 “Particle Analysis”³⁴. Monochrome pictures were taken and a manual threshold was set to separate the cells apart from the background. For particle analysis, minimum and maximum cell area as well as roundness values were selected manually to include as many single cells as possible.

Statistical analysis. Statistical analysis was performed using Prism V6 (GraphPad, La Jolla, CA, USA). Paired statistics were used to analyze sprayed versus unsprayed conditions (paired student's t-test and repeated measurements (RM) two-way analysis of variance (two-way ANOVA) with Bonferroni post-hoc-test). In all other cases one-way analysis of variance (one-way ANOVA) with Tukey's post-hoc-test was performed, unless noted otherwise.

Data Availability

The datasets generated during and/or analyzed during the current study are available from the corresponding author on reasonable request.

References

- Lavin, Y., Mortha, A., Rahman, A. & Merad, M. Regulation of macrophage development and function in peripheral tissues. *Nature reviews Immunology* **15**, 731–744, <https://doi.org/10.1038/nri3920> (2015).
- Ginhoux, F. & Guilliams, M. Tissue-Resident Macrophage Ontogeny and Homeostasis. *Immunity* **44**, 439–449, <https://doi.org/10.1016/j.immuni.2016.02.024> (2016).
- Perdiguer, E. G. *et al.* The Origin of Tissue-Resident Macrophages: When an Erythro-myeloid Progenitor Is an Erythro-myeloid Progenitor. *Immunity* **43**, 1023–1024, <https://doi.org/10.1016/j.immuni.2015.11.022> (2015).
- Mass, E. *et al.* Specification of tissue-resident macrophages during organogenesis. *Science* **353**, <https://doi.org/10.1126/science.aaf4238> (2016).
- van de Laar, L. *et al.* Yolk Sac Macrophages, Fetal Liver, and Adult Monocytes Can Colonize an Empty Niche and Develop into Functional Tissue-Resident Macrophages. *Immunity* **44**, 755–768, <https://doi.org/10.1016/j.immuni.2016.02.017> (2016).
- Lee, S., Kivimae, S., Dolor, A. & Szoka, F. C. Macrophage-based cell therapies: The long and winding road. *J Control Release* **240**, 527–540, <https://doi.org/10.1016/j.jconrel.2016.07.018> (2016).
- Carey, B. & Trapnell, B. C. The molecular basis of pulmonary alveolar proteinosis. *Clinical immunology* **135**, 223–235, <https://doi.org/10.1016/j.clim.2010.02.017> (2010).
- Suzuki, T. *et al.* Hereditary pulmonary alveolar proteinosis: pathogenesis, presentation, diagnosis, and therapy. *Am J Respir Crit Care Med* **182**, 1292–1304, <https://doi.org/10.1164/rccm.201002-0271OC> (2010).
- Bruscia, E. M. & Bonfield, T. L. Cystic Fibrosis Lung Immunity: The Role of the Macrophage. *J Innate Immun* **8**, 550–563, <https://doi.org/10.1159/000446825> (2016).
- Happle, C. *et al.* Pulmonary transplantation of macrophage progenitors as effective and long-lasting therapy for hereditary pulmonary alveolar proteinosis. *Sci Transl Med* **6**, 250ra113, <https://doi.org/10.1126/scitranslmed.3009750> (2014).
- Suzuki, T. *et al.* Pulmonary macrophage transplantation therapy. *Nature* **514**, 450–454, <https://doi.org/10.1038/nature13807> (2014).
- Esteban-Vives, R. *et al.* Calculations for reproducible autologous skin cell-spray grafting. *Burns* **42**, 1756–1765, <https://doi.org/10.1016/j.burns.2016.06.013> (2016).
- Navarro, F. A. *et al.* Sprayed keratinocyte suspensions accelerate epidermal coverage in a porcine microwound model. *J Burn Care Rehabil* **21**, 513–518 (2000).
- Minutti, C. M., Knipper, J. A., Allen, J. E. & Zais, D. M. Tissue-specific contribution of macrophages to wound healing. *Semin Cell Dev Biol* **61**, 3–11, <https://doi.org/10.1016/j.semcdb.2016.08.006> (2017).
- Cannon, G. J. & Swanson, J. A. The macrophage capacity for phagocytosis. *Journal of cell science* **101**(Pt 4), 907–913 (1992).
- Groneberg, D. A., Witt, C., Wagner, U., Chung, K. F. & Fischer, A. Fundamentals of pulmonary drug delivery. *Respir Med* **97**, 382–387 (2003).
- Fischer, M., Koch, W., Windt, H. & Dasenbrock, C. A pilot study on the refinement of acute inhalation toxicity studies: the isolated perfused rat lung as a screening tool for surface-active substances. *Altern Lab Anim* **40**, 199–209 (2012).
- Lootens, L., Brusselaers, N., Beele, H. & Monstrey, S. Keratinocytes in the treatment of severe burn injury: an update. *International wound journal* **10**, 6–12, <https://doi.org/10.1111/j.1742-481X.2012.01083.x> (2013).
- Ter Horst, B., Chouhan, G., Moiemien, N. S. & Grover, L. M. Advances in keratinocyte delivery in burn wound care. *Adv Drug Deliv Rev* **123**, 18–32, <https://doi.org/10.1016/j.addr.2017.06.012> (2018).
- Nathan, C. F. & Hibbs, J. B. Jr. Role of nitric oxide synthesis in macrophage antimicrobial activity. *Current opinion in immunology* **3**, 65–70 (1991).
- Church, D., Elsayed, S., Reid, O., Winston, B. & Lindsay, R. Burn wound infections. *Clin Microbiol Rev* **19**, 403–434, <https://doi.org/10.1128/CMR.19.2.403-434.2006> (2006).
- Hu, M. S. *et al.* Delivery of monocyte lineage cells in a biomimetic scaffold enhances tissue repair. *JCI Insight* **2**, <https://doi.org/10.1172/jci.insight.96260> (2017).
- Heyder, J. Deposition of inhaled particles in the human respiratory tract and consequences for regional targeting in respiratory drug delivery. *Proc Am Thorac Soc* **1**, 315–320, <https://doi.org/10.1513/pats.200409-046TA> (2004).
- Labiris, N. R. & Dolovich, M. B. Pulmonary drug delivery. Part I: physiological factors affecting therapeutic effectiveness of aerosolized medications. *British journal of clinical pharmacology* **56**, 588–599 (2003).
- Menck, K. *et al.* Isolation of human monocytes by double gradient centrifugation and their differentiation to macrophages in teflon-coated cell culture bags. *Journal of visualized experiments: JoVE*, e51554, <https://doi.org/10.3791/51554> (2014).
- Akhoodi, M., Oldenhof, H., Stoll, C., Sieme, H. & Wolkers, W. F. Membrane hydraulic permeability changes during cooling of mammalian cells. *Biochim Biophys Acta* **1808**, 642–648, <https://doi.org/10.1016/j.bbame.2010.11.021> (2011).
- Natan, D., Nagler, A. & Arav, A. Freeze-drying of mononuclear cells derived from umbilical cord blood followed by colony formation. *PloS one* **4**, e5240, <https://doi.org/10.1371/journal.pone.0005240> (2009).
- Buchanan, S. S., Pyatt, D. W. & Carpenter, J. F. Preservation of differentiation and clonogenic potential of human hematopoietic stem and progenitor cells during lyophilization and ambient storage. *PloS one* **5**, <https://doi.org/10.1371/journal.pone.0012518> (2010).
- Ari, A. & Fink, J. B. Differential Medical Aerosol Device and Interface Selection in Patients during Spontaneous, Conventional Mechanical and Noninvasive Ventilation. *J Aerosol Med Pulm Drug Deliv* **29**, 95–106, <https://doi.org/10.1089/jamp.2015.1266> (2016).
- Lachmann, N. *et al.* Large-scale hematopoietic differentiation of human induced pluripotent stem cells provides granulocytes or macrophages for cell replacement therapies. *Stem Cell Reports* **4**, 282–296, <https://doi.org/10.1016/j.stemcr.2015.01.005> (2015).
- Mucci, A. *et al.* Murine iPSC-Derived Macrophages as a Tool for Disease Modeling of Hereditary Pulmonary Alveolar Proteinosis due to Csf2rb Deficiency. *Stem cell reports*, <https://doi.org/10.1016/j.stemcr.2016.06.011> (2016).
- van Wilgenburg, B., Browne, C., Vowles, J. & Cowley, S. A. Efficient, long term production of monocyte-derived macrophages from human pluripotent stem cells under partly-defined and fully-defined conditions. *PLoS One* **8**, e71098, <https://doi.org/10.1371/journal.pone.0071098> (2013).
- Happle, C. *et al.* Pulmonary Transplantation of Human iPSC-derived Macrophages Ameliorates Pulmonary Alveolar Proteinosis. *Am J Respir Crit Care Med*, <https://doi.org/10.1164/rccm.201708-1562OC> (2018).
- Rueden, C. T. *et al.* ImageJ2: ImageJ for the next generation of scientific image data. *BMC Bioinformatics* **18**, 529, <https://doi.org/10.1186/s12859-017-1934-z> (2017).

Acknowledgements

The authors thank Doreen Lüttge and Theresa Buchegger (Hannover Medical School) for excellent technical assistance. Moreover, we would like to thank Prof. Thomas Moritz for critical comments and his support. The authors also thank Daniela Paasch for providing genetically transduced human U937 cells. This work was financially supported by grants from the Deutsche Forschungsgemeinschaft: Cluster of Excellence REBIRTH (Exc 62/2) and the grant LA3680/2-1 (N.L.). The work was also funded by the Helmholtz excellence network REBIRTH4s. Moreover, the work was supported by grants from the Federal Ministry of Education and Research (BMBF iMACnet 01EK1602A), the Else Kröner-Fresenius-Stiftung (EKFS): 2015_92 (N.L.) and 2016_A146 (M.A.). This work was also supported by a scholarship of the REBIRTH PhD program Regenerative Sciences (K.H.).

Author Contributions

V.B. and F.K. designed and performed experiments, analyzed the data and wrote the manuscript; A.L.N., C.H., E.L.R., K.H., A.H.R., J.W.S. and D.W. performed experiments and analyzed data; A.B. and W.W. designed experiments; M.A. designed experiments and wrote the manuscript; N.L. conceived the project, provided financial support and wrote the manuscript. All authors reviewed the manuscript.

Additional Information

Supplementary information accompanies this paper at <https://doi.org/10.1038/s41598-018-34524-2>.

Competing Interests: The authors declare no competing interests.

Publisher's note: Springer Nature remains neutral with regard to jurisdictional claims in published maps and institutional affiliations.



Open Access This article is licensed under a Creative Commons Attribution 4.0 International License, which permits use, sharing, adaptation, distribution and reproduction in any medium or format, as long as you give appropriate credit to the original author(s) and the source, provide a link to the Creative Commons license, and indicate if changes were made. The images or other third party material in this article are included in the article's Creative Commons license, unless indicated otherwise in a credit line to the material. If material is not included in the article's Creative Commons license and your intended use is not permitted by statutory regulation or exceeds the permitted use, you will need to obtain permission directly from the copyright holder. To view a copy of this license, visit <http://creativecommons.org/licenses/by/4.0/>.

© The Author(s) 2018